Development 140, 1364-1368 (2013) doi:10.1242/dev.091844
© 2013. Published by The Company of Biologists Ltd

# *Clear$^{T}$*: a detergent- and solvent-free clearing method for neuronal and non-neuronal tissue

**Takaaki Kuwajima[1], Austen A. Sitko[2], Punita Bhansali[1], Chris Jurgens[3], William Guido[3,‡] and Carol Mason[1,2,*]**

## SUMMARY

We describe a clearing method for enhanced visualization of cell morphology and connections in neuronal and non-neuronal tissue. Using *Clear$^{T}$* or *Clear$^{T2}$*, which are composed of formamide or formamide/polyethylene glycol, respectively, embryos, whole mounts and thick brain sections can be rapidly cleared with minimal volume changes. Unlike other available clearing techniques, these methods do not use detergents or solvents, and thus preserve lipophilic dyes, fluorescent tracers and immunohistochemical labeling, as well as fluorescent-protein labeling.

**KEY WORDS: Clearing reagent, Whole mount, Retinal axon pathway, Immunohistochemistry, Fluorescent protein, DiI**

## INTRODUCTION

Appreciation of neural circuitry and single-cell morphology has benefited from new labeling methods, including fluorescent tracers and genetically encoded fluorescent proteins (Luo et al., 2008). Although these methods produce superb detail of labeled cells and pathways, tissue opacity limits the depth of imaging, necessitating imaging sectioned material in order to attain high microscopic resolution. However, because images must be reconstructed in three dimensions (3D) post-acquisition, imaging and reconstructing sections is neither as efficient nor as accurate as imaging thicker tissue samples.

New reagents that clear or render tissue transparent include Sca*l*e, benzyl-alcohol and benzyl-benzoate (BABB), and a combination of tetrahydrofuran and BABB, all of which preserve genetically expressed fluorescent signal, allowing deep imaging of neural circuitry in 3D (Dodt et al., 2007; Hama et al., 2011; Ertürk et al., 2012). However, these reagents change tissue volume and require several days to weeks to fully clear the tissue (Hama et al., 2011; Ertürk et al., 2012). More importantly, owing to their reliance on detergents or organic solvents, Sca*l*e and BABB disrupt the fluorescent signal of immunohistochemistry, of conventional lipophilic carbocyanine dyes [such as 1,1′-dioctadecyl-3,3,3′,3′-tetramethylindocarbocyanine perchlorate (DiI)] and of fluorescent tracers such as cholera toxin subunit B (CTB). Here, we describe a rapid clearing method that maintains tissue volume and preserves fluorescent signal from tracers, immunohistochemistry and genetically expressed fluorescent proteins.

## MATERIALS AND METHODS

### *Clear$^{T}$* and *Clear$^{T2}$* solutions

For *Clear$^{T}$*, 20%, 40%, 80% and 95% formamide solutions were made by adding formamide (99.6%, considered 100%) (Fisher) to PBS (pH 7.4) (vol/vol).

[1]Department of Pathology and Cell Biology, Columbia University, College of Physicians and Surgeons, 630 West 168th Street, 14-509 P&S, New York, NY 10032, USA. [2]Department of Neuroscience, Columbia University, College of Physicians and Surgeons, 1051 Riverside Drive, New York, NY 10032, USA. [3]Department of Anatomy and Neurobiology,Virginia Commonwealth University, Richmond, VA 23298, USA.

‡Present address: Department of Anatomical Sciences and Neurobiology, School of Medicine, Health Science Center, University of Louisville, Louisville, KY 40202, USA

*Author for correspondence (cam4@columbia.edu)

**Accepted 9 January 2013**

For *Clear$^{T2}$*, a 50% formamide/20% polyethylene glycol (PEG) solution was made by mixing formamide (99.6%, considered 100%, as made for *Clear$^{T}$*) with 40% PEG/$H_2O$ (wt/vol) at a ratio of 1:1 (vol/vol). A 25% formamide/10% PEG solution was made by mixing 50% formamide plus 20% PEG/$H_2O$ (wt/vol) at a ratio of 1:1 (vol/vol). A 40% PEG solution was made by stirring powdered PEG 8000 MW (Sigma-Aldrich) in warm $H_2O$ for 30 minutes, and is stable at room temperature for several months.

### Preparation of specimens and clearing procedures

Procedures for the care and breeding of mice follow regulatory guidelines of the Columbia University Institutional Animal Care and Use Committee. Noon of the day on which a plug was found was considered to be E0.5. C57BL/6J wild-type and *actin*-GFP mouse embryos were removed from mothers anesthetized with ketamine-xylazine (100 and 10 mg/kg, respectively, in 0.9% saline); postnatal wild-type, *Thy1*-GFP (M-line) (a gift from J. A. Gogos, Columbia University, NY, USA) and adult *Tcf/Lef:H2B*-GFP mice (a gift from E. Laufer, Columbia University, NY, USA) were anesthetized with ketamine-xylazine (100 and 10 mg/kg, respectively, in 0.9% saline), fixed in 4% paraformaldehyde (PFA)/PBS (pH 7.4) overnight, or perfused and washed with PBS at 4°C. Embryos were perfused transcardially for optimal clearing. All clearing protocols took place at room temperature.

### *Clear$^{T}$* and *Clear$^{T2}$* tissue-clearing method

Incubation times in each solution vary according to tissue thickness for the desired transparency (see Table 1 for details).

Sca*l*eA2 has been described previously (Hama et al., 2011). E14.5 embryos were cleared with Sca*l*eA2 for 14 days; DiI-labeled embryos or CTB-labeled sections were treated overnight or 2 hours, respectively.

BABB has been described (Dodt et al., 2007). DiI-labeled embryos or CTB-labeled sections were treated with BABB overnight or for 2 hours, respectively, after dehydration with 30%, 50%, 70% and 100% ethanol for 1 hour each and with hexane for 1 hour.

### Retinal axon labeling with DiI and CTB

Anterograde DiI labeling has been described previously (Plump et al., 2002). The eye was placed back into the optic cup and heads were incubated in PBS containing 0.1% sodium azide as follows: E14-E16, 5-7 days at room temperature; E17-P0, 5-7 days at 37°C. The retinogeniculate projection was labeled with CTB as described previously (Jaubert-Miazza et al., 2005; Rebsam et al., 2009), and single neuron labeling in the CTB-labeled dLGN was performed as described previously (Krahe et al., 2011).

### Immunohistochemistry

Vibratome and cryosections were blocked in 5% BSA/1% Tween (Sigma-Aldrich) in PBS (pH 7.4) for 1 hour at room temperature. Mouse monoclonal anti-RC2 (IgM) antibody (Developmental Hybridoma Bank)

**Table 1. Clearing procedures**

A *Clear*$^{T}$

| | Whole embryos or heads | Whole dissected brains (E16-P11) | Half embryonic brains | Sections (20-1000 μm) |
|---|---|---|---|---|
| 20% formamide | 30 minutes | 30 minutes | 30 minutes | 5 minutes |
| 40% formamide | 30 minutes | 30 minutes | 30 minutes | 5 minutes |
| 80% formamide | 2 hours | 2 hours | 2 hours | 5 minutes |
| 95% formamide | 30 minutes | 30 minutes | 30 minutes | 5 minutes |
| 95% formamide | 5-16 hours; E11-E15, respectively | O/N-2 days | 4 hours | 15 minutes |

B *Clear*$^{T2}$

| | Embryonic heads or brains | Sections (20-1000 μm) |
|---|---|---|
| 25% formamide/10% PEG | 1 hour | 10 minutes |
| 50% formamide/20% PEG | 1 hour | 5 minutes |
| 50% formamide/20% PEG | 5-16 hours; E11-E15, respectively | 15-60 minutes |

Incubation times vary with tissue thickness. Time in final buffer can be determined by visual inspection for desired transparency. O/N, overnight.

(1:4) and mouse monoclonal anti-neurofilament (IgG) antibody (2H3) (a gift from T. Jessell and S. Morton, Columbia University, NY, USA) (1:5) were incubated in 1% BSA/1% Tween in PBS overnight at 4°C. After washes with 1% Tween in PBS, Cy3-conjugated anti-mouse IgM and Cy5-conjugated anti-mouse IgG (1:500) secondary antibodies (Jackson) were applied, incubated in 1% BSA/1% Tween in PBS overnight at 4°C. Hoechst 33258 (Molecular Probes) was used for nuclear staining. Whole-mount immunolabeling of embryos with anti-neurofilament antibody has been described previously (Huber et al., 2005).

### Imaging

Whole brains or sections with DiI, CTB or immunolabeling, or sections of GFP-labeled mice were imaged on a Zeiss AxioImager M2 microscope with Apotome, AxioCam MRm camera, Neurolucida software (V10.40, MicroBrightField Systems); with a 5× objective lens (FLUAR, NA=0.25, working distance=12.5 mm), a 20× objective lens (PLAN-APOCHROMAT, NA=0.8, working distance=550 μm) or a 40× objective lens (PLAN-NEOFLUAR, NA=0.75, working distance=710 μm) (Fig. 2B,C; Fig 2D, bottom; Fig. 3C,D,F; supplementary material Fig. S3B, Fig. S4). Using the principle of structured illumination, the Apotome provides confocal-like resolution with epifluorescence imaging. The Apotome improves the signal to noise ratio by acquiring three images of an optical section and subtracting background fluorescence signal. Imaging of whole heads and brains was performed using a Zeiss dissecting microscope StemiSV11, Axiovision software, AxioCam camera (Fig. 1; Fig. 2A; Fig. 3A,B; supplementary material Fig. S1; Fig. S2A). Imaging of whole embryos with immunolabeling was performed using Nikon SMZ 1500 zoom stereomicroscope and DS-Qi1Mc camera (Fig. 3E). A Zeiss Axioplan 2 microscope, AxioCam camera and Axiovision software was used to image thin brain sections using a 10× objective lens (PLAN-NEOFLUAR, NA=0.3) or a 20× objective lens (PLAN-NEOFLUAR, NA=0.5) (supplementary material Fig. S2B, Fig. S3A, Fig. S5). Thick samples were imaged using a home-made slide to keep tissue submerged in formamide solutions and covered with a regular glass coverslip: a square rim of plastic or silicone elastomer was super-glued to a regular glass slide.

### Statistical analysis

All experiments were performed three or more times with similar results. Data were analyzed and graphs constructed using Metamorph or Microsoft Excel. Error bars represent s.e.m. and statistical analysis was performed using Student's *t*-test; $P>0.05$ indicates non-significance.

## RESULTS AND DISCUSSION

### *Clear*$^{T}$ is a rapid tissue clearing method

After observing that 20 μm cryosections of embryonic mouse brain became transparent in the hybridization buffer used for *in situ* hybridization, we found that a component of the buffer, formamide, could clear thick tissue samples. Here, we demonstrate the versatility of our method, named *Clear*$^{T}$ for neuronal and non-neuronal tissue, and compare its clarity, rapidity and tissue expansion/shrinkage to existing clearing methods.

Intact embryos, embryonic and postnatal dissected heads, brains, and thick (up to 1000 μm) brain sections, were fixed and sequentially immersed in graded concentrations of formamide (Table 1A, Fig. 1A). The *Clear*$^{T}$ procedure rendered embryonic brains as transparent as with Sca*l*eA2, but did so significantly faster (1 day versus 14 days) (Fig. 1B). Completely cleared postnatal day 0 (P0) brain sections were similar to their original size (before clearing=1.0±0 versus *Clear*$^{T}$=1.04±0.02, not significant, $n$=6 sections) (Fig. 1C). Even after prolonged treatment with *Clear*$^{T}$, sample volume only increased slightly, significantly less than in Sca*l*eA2 [1 day, *Clear*$^{T}$=1.33±0.09 versus Sca*l*eA2=1.81±0.05, $P<0.01$; 2 days, *Clear*$^{T}$=1.27±0.09 versus Sca*l*eA2=1.83±0.06, $P<0.01$, $n$=5 (*Clear*$^{T}$), 4 (Sca*l*eA2) sections] (supplementary material Fig. S1). Although formamide is not harmful to tissue in the short term, it is unsuitable for long-term tissue storage. Therefore,

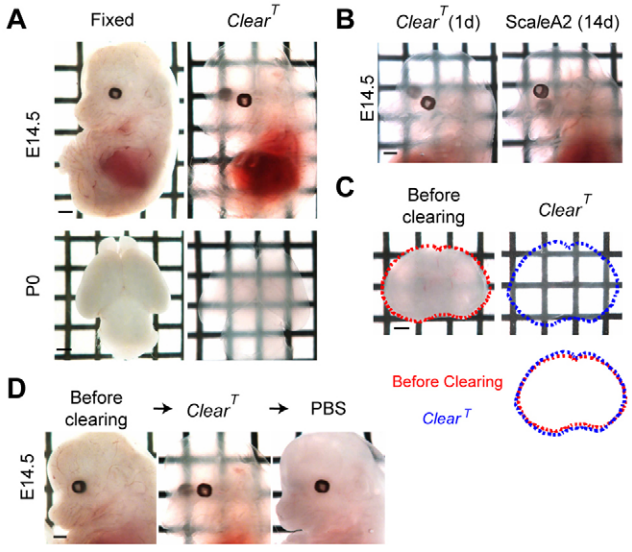


**Fig. 1. Rapid tissue clearing with *Clear*$^{T}$.** (**A**) Fixed whole embryos (E14.5) and dissected postnatal brains (P0) were cleared overnight. The grid is visible through tissue cleared by *Clear*$^{T}$. (**B**) E14.5 embryos cleared with *Clear*$^{T}$ or Sca*l*eA2 reach full transparency in 1 day or 14 days, respectively. (**C**) *Clear*$^{T}$ does not lead to volume changes. P0 sections (800 μm), surface area measured: pre-cleared, red line; *Clear*$^{T}$, blue line. (**D**) Clearing is reversible with PBS (30 minutes). Scale bars: 1 mm.

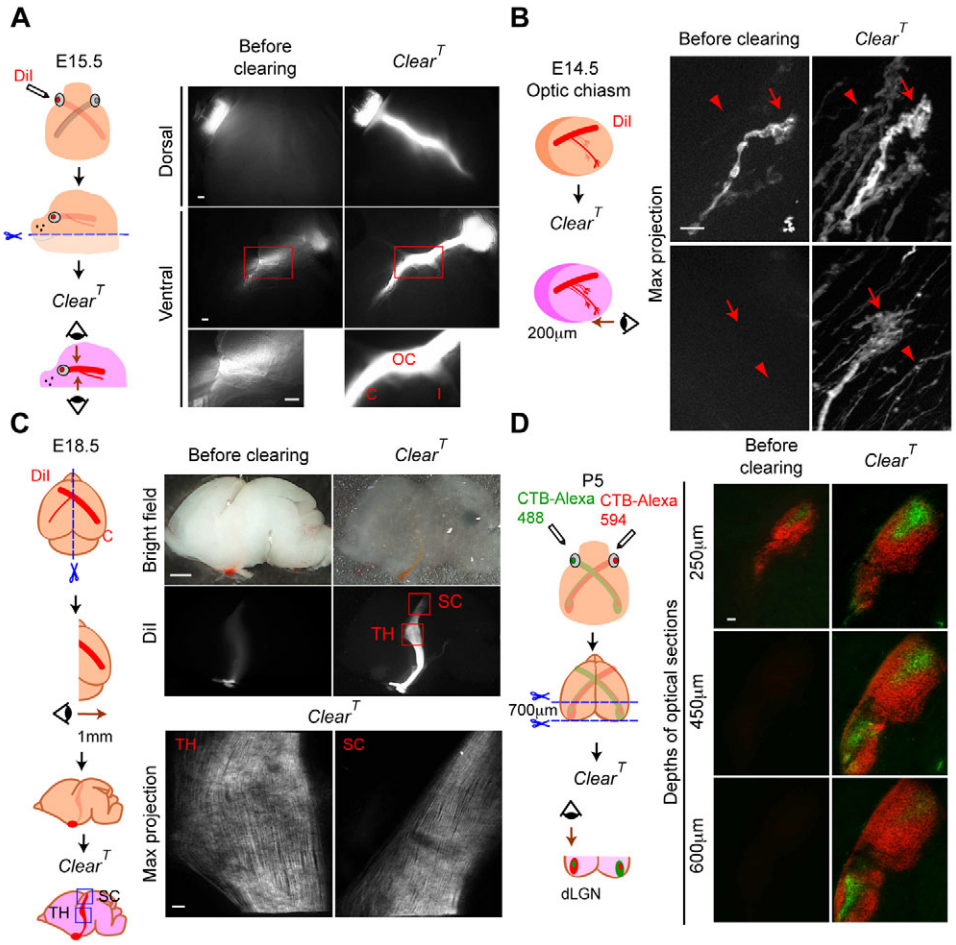


**Fig. 2. Retinal axon projections in brain tissue cleared with *Clear*$^{T}$.** (**A**) E15.5 eye was labeled with DiI, the jaw and tongue were cut away and the head was cleared with *Clear*$^{T}$. DiI-labeled contralateral (C) and ipsilateral (I) retinal axons and optic chiasm are detected in both dorsal and ventral views after clearing with *Clear*$^{T}$. (**B**) Merged stack (41 images, 5 µm steps) of E14.5 DiI-labeled growth cones (GCs) (arrows) and axons (arrowheads) of the ipsilateral optic tract; imaged from the ventral surface of 200 µm brain section, before and after clearing. (**C**) DiI-labeled contralateral RGC projection to the thalamus and superior colliculus at E18.5. Brains were cut sagittally at the midline and cleared with *Clear*$^{T}$. Merged stack (51 images, 20 µm steps), viewed from the midline. DiI-labeled RGC axons in the dLGN in the thalamus (TH) and superior colliculus (SC) were undetectable in pre-cleared tissue, but easily visible after clearing. (**D**) CTB conjugated to Alexa Fluor 488 or 594 was injected into each eye and a 700 µm frontal section of P5 brain was cleared with *Clear*$^{T}$. Optical slices at 250 µm, 450 µm and 600 µm below the tissue section surface are shown (from 71 images, 10 µm steps). Both CTB labels were observable, though deeper, in cleared dLGN compared with the same tissue before clearing. Scale bars: 1 mm in C (top); 100 µm in A and bottom of C,D (bottom); 10 µm in B.

we transferred samples treated with *Clear*$^{T}$ into PBS, where they became opaque within 30 minutes and could be safely stored for at least 1 month (Fig. 1D).

## Visualization of DiI- or CTB-labeled axons in tissue cleared with *Clear*$^{T}$

The projections, connections, and growth cone (GC) morphology of developing axons can be visualized by anterograde labeling with lipophilic dyes (Little et al., 2009; Bielle et al., 2011). Here, we use the mouse visual system, a classic model for studying neural circuitry development, to demonstrate the advantages of clearing the mouse brain with *Clear*$^{T}$ in preserving lipophilic fluorescent dye labeling. We anterogradely labeled retinal ganglion cell (RGC) axons in embryonic day (E) 14.5 embryos with DiI and treated embryos with *Clear*$^{T}$, Sca*l*eA2 or BABB for 1 day. DiI labeling of retinal axons in the optic nerve and chiasm was preserved after treatment with *Clear*$^{T}$, but treatment with either Sca*l*eA2 or BABB degraded the fluorescent signal (supplementary material Fig. S2A).

We then examined DiI-labeled RGC axons in cleared tissue at the optic chiasm at E15.5 (Fig. 2A). The DiI-labeled retinal projection was not visible prior to clearing, but could be seen through both dorsal and ventral aspects of the cleared head, with jaw and tongue removed but skin and skull intact (Fig. 2A). We examined the resolution of fine morphological detail of DiI-labeled axons and GCs in the proximal ipsilateral optic tract at E14.5 before and after clearing (Fig. 2B). The number and resolution of DiI-labeled axons and GC processes (e.g. filopodia and lamellopodia) were markedly increased after clearing with *Clear*$^{T}$ (Fig. 2B). Furthermore, E18.5 DiI-labeled RGC axons in the thalamus and superior colliculus were not visible before clearing when imaged from the midline of parasagittal hemisections, but the full tract was distinctly visible after clearing with *Clear*$^{T}$, even through a depth of ~1 mm (Fig. 2C).

CTB is widely used for the analysis of postnatal RGC axon targeting in the dLGN (Jaubert-Miazza et al., 2005; Rebsam et al., 2009). To test the compatibility of CTB with *Clear*$^{T}$, we anterogradely labeled each eye of P5 pups with CTB conjugated to either Alexa Fluor 488 or 594. CTB labeling was preserved after *Clear*$^{T}$ and BABB treatments, but BABB reduced tissue size by half (before clearing=1±0 versus cleared=0.50±0.02, $P<0.05$, $n=4$ sections), while labeling was diffuse following Sca*l*eA2 treatment (supplementary material Fig. S2B). CTB labeling was visible through the entire depth of a 700 µm section of P5 brain treated with *Clear*$^{T}$, whereas fluorescence could not be seen beyond 250 µm before clearing (Fig. 2D). Moreover, it is possible to successively clear, unclear (in PBS) and re-clear DiI- or CTB-labeled samples without compromising tissue or label integrity (supplementary material Fig. S3A,B).

## *Clear*$^{T2}$ clears tissue with fluorescent protein and with immunohistochemical label

Our original *Clear*$^{T}$ protocol diminished green fluorescent protein (GFP) intensity in E14.5 *actin*-GFP embryos (Ikawa et al., 1995). Because polyethylene glycol (PEG) stabilizes protein conformation (Rawat et al., 2010), we investigated whether PEG would stabilize GFP expression in formamide. Whereas 50% formamide failed to

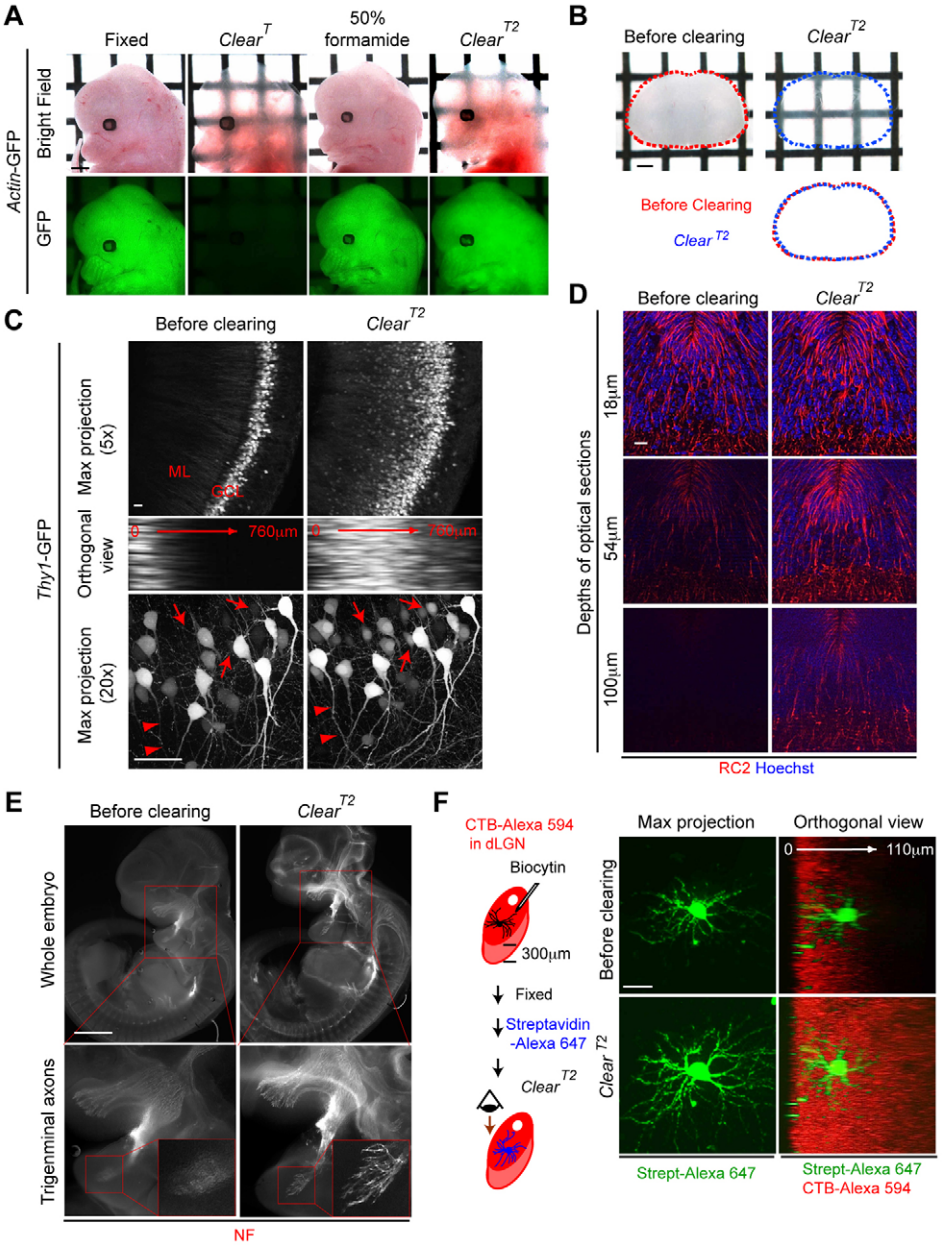


**Fig. 3. *Clear*$^{T2}$ clears tissue with fluorescent proteins or immunohistochemistry.** (**A**) *Clear*$^{T}$ cleared E14.5 *actin-GFP* embryos, but reduced GFP fluorescence. Formamide (50%) maintained fluorescence, but failed to clear embryos. *Clear*$^{T2}$ cleared embryos and maintained fluorescence. (**B**) P0 sections (800 µm) were transparent after *Clear*$^{T2}$, with no volume change. (**C**) P11 *Thy1*-GFP (M-line) hippocampus section (800 µm), before and after clearing with *Clear*$^{T2}$; 38 images, 20 µm steps (top and middle). GFP$^{+}$ pyramidal neurons (arrows) and dendrites (arrowheads) in CA1 region are markedly more visible after clearing; 52 images, 2.5 µm steps (bottom). GCL, granule cell layer; ML, molecular layer. (**D**) Sections of E14.5 optic chiasm (200 µm), immunolabeled with the radial glial marker RC2, cleared with *Clear*$^{T2}$; 51 images, 3 µm steps; three optical slices shown. RC2$^{+}$ staining was observed deeper in cleared compared with pre-cleared tissue. Blue indicates Hoechst staining. (**E**) E11.5 whole embryos, immunolabeled with neurofilament antibody (NF) and treated with *Clear*$^{T2}$. NF$^{+}$ axons were much more visible in cleared embryos (top); magnification of trigeminal axons reaching epithelial targets (bottom). (**F**) Section (300 µm) of postnatal mouse brain, dLGN anterogradely labeled with CTB conjugated to Alexa Fluor 594. A single neuron was filled with biocytin and immunostained with streptavidin-Alexa Fluor 647. Clearing with *Clear*$^{T2}$ enhanced resolution and visibility of the dendritic arbor of the neuron. Merged stack, 55 images, 2 µm steps. CTB label is in red; biocytin-filled neuron is pseudo-colored green. Scale bars: 1 mm in A,B,E; 40 µm in C; 20 µm in D,F.

clear brains, a 20% PEG/50% formamide mixture successfully cleared brain tissue and preserved fluorescence. This modified method, named *Clear*$^{T2}$, also requires immersion in a graded series of formamide/PEG solutions (25% formamide/10% PEG then 50% formamide/20% PEG) (Table 1B, Fig. 3A). Although tissue transparency with *Clear*$^{T2}$ was less complete than with *Clear*$^{T}$, application of *Clear*$^{T2}$ induced robust transparency of thick P0 brain sections without volume changes (before clearing=1.0 versus *Clear*$^{T2}$=0.98±0.02, $n$=6, not significant) (Fig. 3B). Sections treated with *Clear*$^{T2}$ for 1 or 2 days were slightly larger than pre-cleared sections, but these changes were significantly less than with Sca*l*eA2 [1 day, *Clear*$^{T2}$=1.30±0.02 versus Sca*l*eA2=1.81±0.05, $P$<0.01; 2 days, *Clear*$^{T2}$=1.30±0.01 versus Sca*l*eA2=1.83±0.06, $P$<0.01, $n$=6 (*Clear*$^{T2}$), $n$=4 sections (Sca*l*eA2)] (supplementary material Fig. S1). *Clear*$^{T2}$ also maintained DiI and CTB labeling in axons as successfully as *Clear*$^{T}$ (supplementary material Fig. S2A,B).

We next examined whether neurons genetically labeled with fluorescent proteins, such as in *Thy1*-GFP (M-line) mice (Feng et al., 2000), could be visualized with *Clear*$^{T2}$ (Fig. 3C). After clearing thick hippocampal sections with *Clear*$^{T2}$, *Thy1*-GFP$^{+}$ neurons were visible deeper within the granule cell layer (Fig. 3C, top) and details of GFP$^{+}$ pyramidal neuron dendrites in the CA1 region were more distinct than without clearing (Fig. 3C, bottom). To determine whether *Clear*$^{T2}$ could be applied to adult or non-neuronal tissue, we used *Tcf/Lef:H2B*-GFP mice, in which reporter expression is detected in neuronal and non-neuronal tissues from early embryonic to adult stages (Ferrer-Vaquer et al., 2010). H2B-GFP nuclear labeling in neurons of the cerebral cortex, cells within the granule cell and molecular layers of the hippocampus, progenitor cells of the small intestine and satellite cells of skeletal muscle were more apparent after clearing with *Clear*$^{T2}$ (supplementary material Fig. S4).

Immunohistochemistry is used to visualize protein expression, but labeling is usually visible only superficially in thick tissue sections. To examine whether immunohistochemistry labeling is compatible with tissue clearing, we immunostained E14.5

cryosections through the optic chiasm with an antibody to the radial glia marker RC2 and treated sections with *Clear$^{T}$*, *Clear$^{T2}$*, Sca*l*eA2 or BABB (supplementary material Fig. S5A,B). *Clear$^{T}$* and Sca*l*eA2 disrupted RC2 immunolabeling, and BABB maintained fluorescent signal but produced labeling artifacts in bone and cell nuclei that should not express RC2. As *Clear$^{T2}$* successfully preserved immunolabeling (supplementary material Fig. S5A-E), we applied it to 200 μm RC2-immunolabeled vibratome sections of the optic chiasm at E14.5 (Fig. 3D). RC2$^{+}$ glial processes were visible as deep as ~120 μm in cleared tissue, twice as deep as in pre-cleared tissue (Fig. 3D). Finally, *Clear$^{T2}$* treatment of whole mouse embryos immunostained with an antibody to neurofilament (NF) provided a complete view of axon tracts and arbors in the CNS and PNS in distal appendages (Fig. 3E).

Finally, we examined whether *Clear$^{T2}$* is compatible with multiple fluorescent labels. After applying *Clear$^{T2}$* to a thick brain section with CTB-labeled dLGN, a biocytin-filled relay neuron was visualized more deeply and at higher resolution than before clearing, with both labels successfully maintained (Fig. 3F).

## *Clear$^{T}$* and *Clear$^{T2}$* are solvent- and detergent-free rapid tissue clearing methods

We have developed two clearing methods, *Clear$^{T}$* and *Clear$^{T2}$*, which aid analysis of fluorescent labeling in embryonic and mature neuronal and non-neuronal tissue. *Clear$^{T2}$* clears specimens while effectively maintaining the fluorescent signal of genetically encoded proteins, immunohistochemistry labeling, and dye tracers such as DiI and CTB. Whereas *Clear$^{T}$* is incompatible with immunohistochemistry and genetically encoded fluorescence proteins (supplementary material Table S1), transparency of whole brains treated with *Clear$^{T}$* is better than with *Clear$^{T2}$* (Fig. 3A). Therefore, tissue samples labeled with DiI or CTB alone are best cleared by *Clear$^{T}$*.

*Clear$^{T}$* and *Clear$^{T2}$* provide several advantages over other available clearing methods. Clearing time for thick sections, whole brains or embryos is significantly faster than with Sca*l*eA2 or BABB. In addition, *Clear$^{T}$* and *Clear$^{T2}$* produce minimal tissue volume changes, significantly less than Sca*l*eA2 or BABB. Most importantly, our methods maintain DiI- and CTB-labeling in axons, unlike Sca*l*eA2 and BABB (supplementary material Table S1). *Clear$^{T}$* and *Clear$^{T2}$* successfully clear postnatal and adult brain and other tissues. *Clear$^{T2}$* provides a final important advantage over Sca*l*eA2 and BABB, in that it can clear immunolabeled tissue. Thus, *Clear$^{T}$* and *Clear$^{T2}$* provide improved clearing of embryonic and adult neuronal and non-neuronal tissue for viewing fluorescent labeling of cells and fiber tracts by high-resolution optical imaging.

**Acknowledgements**

We thank members of the Mason lab and Columbia University colleagues, Wes Grueber for advice and reading the manuscript, Joseph Gogos for *Thy1*-GFP (M-line) mice, Ed Laufer for *Tcf/Lef:H2B*-GFP mice, and Tom Jessell and Susan Morton for the anti-neurofilament antibody. Thomas E. Krahe in William Guido's laboratory produced additional slice preparations of biocytin-filled cells in the dLGN (not shown).

**Funding**

This work was supported by the National Institues of Health [R01 EY012736 and EY015290 to C.M., T32 EY013933 to A.A.S. and R01 EY012716 to W.G.] and the Uehara Foundation (T.K.). Deposited in PMC for release after 12 months.

**Competing interests statement**

The authors declare no competing financial interests.

**Supplementary material**

Supplementary material available online at
http://dev.biologists.org/lookup/suppl/doi:10.1242/dev.091884/-/DC1

**References**

**Bielle, F., Marcos-Mondéjar, P., Leyva-Díaz, E., Lokmane, L., Mire, E., Mailhes, C., Keita, M., García, N., Tessier-Lavigne, M., Garel, S. et al.** (2011). Emergent growth cone responses to combinations of Slit1 and Netrin 1 in thalamocortical axon topography. *Curr. Biol.* **21**, 1748-1755.

**Dodt, H. U., Leischner, U., Schierloh, A., Jährling, N., Mauch, C. P., Deininger, K., Deussing, J. M., Eder, M., Zieglgänsberger, W. and Becker, K.** (2007). Ultramicroscopy: three-dimensional visualization of neuronal networks in the whole mouse brain. *Nat. Methods* **4**, 331-336.

**Ertürk, A., Mauch, C. P., Hellal, F., Förstner, F., Keck, T., Becker, K., Jährling, N., Steffens, H., Richter, M., Hübener, M. et al.** (2012). Three-dimensional imaging of the unsectioned adult spinal cord to assess axon regeneration and glial responses after injury. *Nat. Med.* **18**, 166-171.

**Feng, G., Mellor, R. H., Bernstein, M., Keller-Peck, C., Nguyen, Q. T., Wallace, M., Nerbonne, J. M., Lichtman, J. W. and Sanes, J. R.** (2000). Imaging neuronal subsets in transgenic mice expressing multiple spectral variants of GFP. *Neuron* **28**, 41-51.

**Ferrer-Vaquer, A., Piliszek, A., Tian, G., Aho, R. J., Dufort, D. and Hadjantonakis, A. K.** (2010). A sensitive and bright single-cell resolution live imaging reporter of Wnt/ß-catenin signaling in the mouse. *BMC Dev. Biol.* **10**, 121.

**Hama, H., Kurokawa, H., Kawano, H., Ando, R., Shimogori, T., Noda, H., Fukami, K., Sakaue-Sawano, A. and Miyawaki, A.** (2011). Scale: a chemical approach for fluorescence imaging and reconstruction of transparent mouse brain. *Nat. Neurosci.* **14**, 1481-1488.

**Huber, A. B., Kania, A., Tran, T. S., Gu, C., De Marco Garcia, N., Lieberam, I., Johnson, D., Jessell, T. M., Ginty, D. D. and Kolodkin, A. L.** (2005). Distinct roles for secreted semaphorin signaling in spinal motor axon guidance. *Neuron* **48**, 949-964.

**Ikawa, M., Kominami, K., Yoshimura, Y., Tanaka, K., Nishimune, Y. and Okabe, M.** (1995). A rapid and non-invasive selection of transgenic embryos before implantation using green fluorescent protein (GFP). *FEBS Lett.* **375**, 125-128.

**Jaubert-Miazza, L., Green, E., Lo, F. S., Bui, K., Mills, J. and Guido, W.** (2005). Structural and functional composition of the developing retinogeniculate pathway in the mouse. *Vis. Neurosci.* **22**, 661-676.

**Krahe, T. E., El-Danaf, R. N., Dilger, E. K., Henderson, S. C. and Guido, W.** (2011). Morphologically distinct classes of relay cells exhibit regional preferences in the dorsal lateral geniculate nucleus of the mouse. *J. Neurosci.* **31**, 17437-17448.

**Little, G. E., López-Bendito, G., Rünker, A. E., García, N., Piñon, M. C., Chédotal, A., Molnár, Z. and Mitchell, K. J.** (2009). Specificity and plasticity of thalamocortical connections in Sema6A mutant mice. *PLoS Biol.* **7**, e98.

**Luo, L., Callaway, E. M. and Svoboda, K.** (2008). Genetic dissection of neural circuits. *Neuron* **57**, 634-660.

**Plump, A. S., Erskine, L., Sabatier, C., Brose, K., Epstein, C. J., Goodman, C. S., Mason, C. A. and Tessier-Lavigne, M.** (2002). Slit1 and Slit2 cooperate to prevent premature midline crossing of retinal axons in the mouse visual system. *Neuron* **33**, 219-232.

**Rawat, S., Raman Suri, C. and Sahoo, D. K.** (2010). Molecular mechanism of polyethylene glycol mediated stabilization of protein. *Biochem. Biophys. Res. Commun.* **392**, 561-566.

**Rebsam, A., Petros, T. J. and Mason, C. A.** (2009). Switching retinogeniculate axon laterality leads to normal targeting but abnormal eye-specific segregation that is activity dependent. *J. Neurosci.* **29**, 14855-14863.